LETTERS

Direct observation of steps in rotation of the bacterial flagellar motor

Yoshiyuki Sowa[1]*, Alexander D. Rowe[2]*, Mark C. Leake[2], Toshiharu Yakushi[3], Michio Homma[3], Akihiko Ishijima[1,4] & Richard M. Berry[2]

The bacterial flagellar motor is a rotary molecular machine that rotates the helical filaments that propel many species of swimming bacteria[1,2]. The rotor is a set of rings up to 45 nm in diameter in the cytoplasmic membrane[3]; the stator contains about ten torque-generating units anchored to the cell wall at the perimeter of the rotor[4,5]. The free-energy source for the motor is an inward-directed electrochemical gradient of ions across the cytoplasmic membrane, the protonmotive force or sodium-motive force for H^+-driven and Na^+-driven motors, respectively. Here we demonstrate a stepping motion of a Na^+-driven chimaeric flagellar motor in *Escherichia coli*[6] at low sodium-motive force and with controlled expression of a small number of torque-generating units. We observe 26 steps per revolution, which is consistent with the periodicity of the ring of FliG protein, the proposed site of torque generation on the rotor[7,8]. Backwards steps despite the absence of the flagellar switching protein CheY indicate a small change in free energy per step, similar to that of a single ion transit.

Direct observation of steps in ATP-driven molecular motors has revealed much about the fundamental mechanisms of these protein machines[9–11]. Steps characteristic of the ATP-driven F_1 part of ATP synthase have been observed when the whole enzyme is driven by ion flow in the F_O part[12], but steps have never been seen in a purely ion-driven molecular machine. Steps have not previously been resolved in the flagellar motor[13] because of its high speed[14,15], the presence of multiple stator units in a single motor[4] and the small step size predicted—either from structural data on rotor periodicity or from mechanical data obtained by dividing the free energy of one ion crossing the membrane by the torque that the motor generates. We took several measures to overcome these factors. We detected rotation by back-focal-plane (BFP) interferometry of 500-nm diameter polystyrene beads attached to spontaneously sticky flagellar filaments of *E. coli*, as described previously[16], or by high-speed video recording of 200-nm fluorescent beads attached in the same way (Fig. 1b, c, inset). The structure and function of H^+ and Na^+ motors are similar, and functional chimaeras have been made containing different mixtures of H^+ and Na^+ motor components[17]. We slowed motor rotation to the point at which steps could be resolved by decreasing the sodium-motive force (SMF) in *E. coli* cells containing Na^+-driven chimaeric motors (in which the H^+-driven stator proteins MotA and MotB are replaced by the Na^+-driven PomA and the chimaeric fusion protein PotB, respectively[6]; Fig. 1a). We decreased the SMF by a low external Na^+ concentration in experiments with BFP detection and by cumulative photodamage in fluorescence experiments. We controlled the number of stator units by inducible expression of stator proteins in a strain with wild-type stator proteins deleted. We also deleted *cheY* and *pilA* to avoid possible complications due to motor switching or sticking of beads to cell bodies, respectively. We obtained rotation speed by means of power spectra of the combined x and y signals[16], and bead angles by modelling the raw data as the projection of an oblique circular orbit[18].

Fast Na^+-dependent rotation and reduced speed when Li^+ replaced Na^+ (data not shown) indicate that the chimaera behaves as a typical Na^+ motor[15,19]. For step experiments, we grew cells with low inducer levels to produce fully energized motors with a small initial number of stator units (typically three or four; Supplementary Information). Reduction of the SMF, either by lowering the Na^+ concentration in BFP experiments (Supplementary Information) or by photodamage in fluorescence experiments, led to a decrease in both the number of stator units and the speed per unit. Figure 1b shows the speed of a 500-nm bead in a typical BFP experiment. The Na^+ concentration was reduced from 5 mM to 0.1 mM for the interval between the black arrows, during which the motor rotated at about 1 Hz. This cell rotated with four stator units when first observed in 5 mM Na^+, but this number was decreased to one by a previous reduction of $[Na^+]$ (data not shown). Discrete speed increments identical to those occurring after the induced expression of stator proteins[16] were typical during recovery after the transient

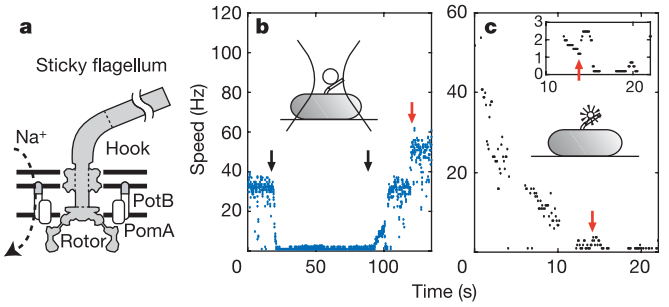

Figure 1 | Rotation measurements of chimaeric Na^+-driven flagellar motors in *E. coli*. **a**, Diagram of the Na^+-driven chimaeric flagellar motor. Components derived from *V. alginolyticus* (stators; PomA, PotB) and *E. coli* (PotB, rotor) are indicated in white and grey, respectively. **b**, Reducing SMF and motor speed by lowering the external Na^+ concentration (from 5 mM to 0.1 mM and back; black arrows), with BFP detection (inset). **c**, Reducing SMF and motor speed by photodamage, with fluorescent detection (inset, lower).The speed doublings in **b** and **c** (red arrows; shown with expanded scales in **c**, inset, top) indicate a change from one to two stators. Data window lengths are 1 s (main figures) and 4 s (inset).

[1]Department of Applied Physics, Graduate School of Engineering, Nagoya University, Furo-cho, Chikusa-ku, Nagoya, Aichi 464-8603, Japan. [2]The Clarendon Laboratory, Department of Physics, Oxford University, Parks Road, Oxford OX1 3PU, UK. [3]Division of Biological Science, Graduate School of Science, Nagoya University, Furo-cho, Chikusa-ku, Nagoya, Aichi 464-8602, Japan. [4]PRESTO, Japan Science and Technology Corporation (JST) 4-1-8, Honmachi, Kawagoe, Saitama 332-0012, Japan.
*These authors contributed equally to this work.

removal of Na^+(Fig. 1b), indicating reversible inactivation of stator units on disruption of the SMF. Similar phenomena have been reported for H^+-driven motors of *E. coli*[20] and *Rhodobacter sphaeroides*[21]. Figure 1c shows the speed of a 200-nm fluorescent bead in a typical fluorescence experiment. We attribute periods of smooth speed reduction to photodamage-induced reduction of the membrane voltage[22], and discrete speed changes (inset) to the consequent reversible inactivation of stator units. Speed doublings such as those in Fig. 1b, c were interpreted as a change from one to two stators. However, faster speed fluctuations were common and we were not always able to assign a definite stator number.

Figure 2a shows a sequence of images of a rotating 200-nm fluorescent bead with calculated bead centres superimposed (Methods). Figure 2b shows stepping rotation of 500-nm plain and 200-nm fluorescent beads attached to chimaeric flagellar motors. The diameter of bead orbits (insets) is consistent with attachment to a short flagellar filament stub. Steps were detected at speeds below 7 and 40 Hz in BFP and fluorescence experiments, respectively, and were not restricted to episodes with an estimated single stator unit. Figure 3a shows expanded sections of the traces in Fig. 2b (more examples are given in Supplementary Information), with the output of a step-finding algorithm (Methods) superimposed. Backwards steps were observed in both BFP and fluorescence experiments, with higher probability at lower speeds. As the strain lacks the switch-inducing protein CheY and never rotated backwards at high Na^+ concentration, backwards steps represent microscopic reversibility rather than motor switching. Similar steps have been seen, although less frequently, in ATP-driven molecular motors[10,11]. Figure 3b shows several revolutions of a 200-nm bead, the histogram of all dwell angles during those revolutions and the power spectrum of that histogram. The peak at 26 per revolution in the spectrum corresponds to steps of 13.8° and indicates that successive revolutions show the same stopping angles.

We combined and analysed step data from different cells and both experimental techniques. Figure 4a shows the step-size histogram for all steps found. Assuming that larger steps are in fact unresolved multiple steps, we fit the distribution as a sum of gaussian distributions with means equal to integer multiples of step size, allowing different sizes and variances for forward and backward fits. The fitted step sizes are 13.7° (26 per revolution) and −10.3° (35 per revolution) for forward and backward steps, respectively. The difference between step sizes may be due to reorientation of the rotation axis on reversal, or it may be an artefact of measurement and analysis. Figure 4b shows the sum of histogram power spectra, similar to those of Fig. 3b, for all step data. Histograms of the levels between steps found by the step algorithm were also made; the sum of their power spectra is shown in the inset to Fig. 4b. The most striking peak is at 26 per revolution, with others at 11, 16 and 23 per revolution. After subdivision of the data, neither step size nor periodicity depended on the individual cell, experimental method, angle, estimated number of stator units or average speed of rotation.

Stepping motion in ATP-driven molecular motors reflects both the discrete molecular nature of the fuel and the periodicity of the 'track' along which the motor runs[9–12]. Our observation of 26 steps per

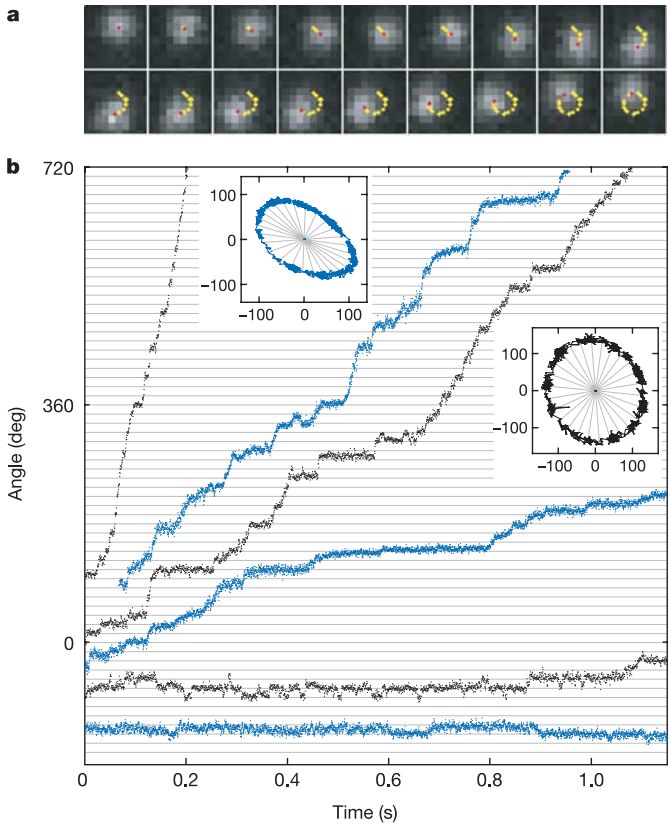

Figure 2 | Stepping rotation. a, Selected frames at 21-ms intervals during one rotation of a 200-nm fluorescent bead. Red and yellow dots mark the calculated bead centre in the current and previous images respectively. Each pixel is 80 nm square. **b**, Stepping rotation of flagellar motors with a range of average speeds. Bead positions are shown in the insets (scales in nanometres); bead angles are plotted against time in the main figure. Grey lines indicate (360/26)° in both main and inset figures. Blue and black traces are from BFP and fluorescence experiments, respectively. Backwards and forwards steps were observed at all speeds.

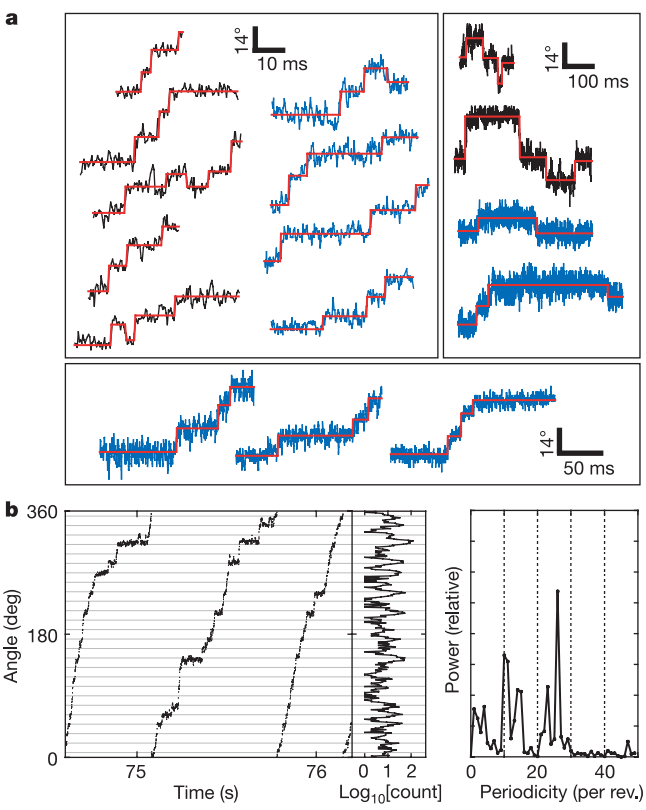

Figure 3 | Analysis of step size and periodicity. a, Selected sections of the traces in Fig. 2b, with the output of a step-finding algorithm superimposed (red). Blue and black traces are from BFP and fluorescence experiments, respectively, as in Fig. 2b. The dominant step size is about 14°. **b**, Plot of angle against time during three revolutions of a 200-nm bead, a histogram of dwell angles for the same revolutions and the power spectrum of that histogram. The peak at 26 per revolution corresponds to a step size of 13.8°, and shows that the motor stops at the same angles on successive revolutions.

revolution is consistent with the periodicity of the ring of FliG protein, the track on the rotor where torque is generated[7,8]. The 10-fold or 11-fold periodicity matches the filament and hook[23]; other periodicities observed may be due to interactions between other components of the flagellum with as-yet undetermined symmetry. Some cells in BFP experiments rotated at about 1 Hz even in 5 mM Na^+. Steps were seen in these unusually slow episodes (data not shown), similar to or possibly slightly smaller than 1/26 of a revolution. Locking of one stator in one state of its mechanochemical cycle while other stators continued normally could produce steps with the periodicity of the locked state. Unusually slow episodes are excluded from our data analysis, but we cannot entirely rule out a possible contribution of a locking effect. Interval length distributions for data with a narrow range of average speed were sometimes, but not always, single-exponential. The apparent independence of step size on stator number, non-exponential interval length distributions and the observation of occasional steps smaller than 1/26 of a revolution may require the revision of existing models of the flagellar motor as a set of independent poisson-stepping stators[16,24].

Our experiments cannot determine whether single steps correspond to single ion transits. Regardless of the nature of the stepping process, the ratio of forwards to backwards step probabilities is $\exp(-\Delta G/kT)$, where ΔG is the free energy available to drive one step and kT is the average thermal energy. In our experiments ΔG ranged from 0 to $3kT$, depending on rotation speed. This is equivalent to the free energy of one ion transit through a SMF of up to −75 mV. Measuring the SMF in *E. coli* under these conditions would reveal whether the observed steps could be driven by single-ion transits. However, previous data indicate that single ions in fully energized wild-type motors cannot drive steps as large as 14°. If about ten torque-generating units pass 1,200 H^+ ions per revolution[25], then one ion in one unit should step about 3°, assuming tightly coupled independent units[16]. Energy conservation sets an upper bound to the angle coupled to one ion transit, equal to (free energy per ion)/(maximum torque per unit). A wild-type *E. coli* cell with a protonmotive force of about 150 mV ($6kT$ per ion)[26] drives a 1-μm bead with an estimated 280 pN nm per unit[16], giving an upper bound of about 5°. It is possible that stoichiometry changes at low SMF or stator number or that smaller substeps will be resolved in future. Alternatively, a mechanical step may be coupled to several ion transits, requiring the accumulation either of ions or of mechanical strain between steps. The latter mechanism is believed to occur in ATP-synthase, coupling three or four ion-driven steps in F_O to a single ATP-synthesizing step in F_1. By combining high-resolution measurements of flagellar rotation with manipulation of the SMF, the chimaeric flagellar motor described here will enable a detailed comparison to be made between the mechanism of the bacterial flagellar motor and those of its ATP-driven relatives.

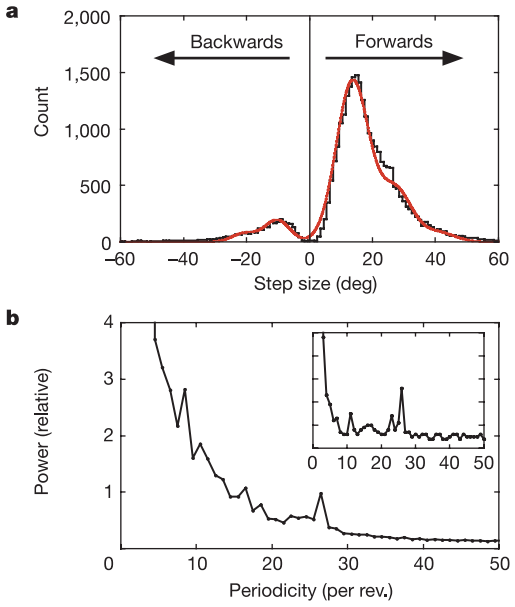

Figure 4 | Summary of step analysis. a, A histogram of step sizes found in all episodes of approximately constant speed (1,400 revolutions, 9 different cells, 28,611 steps). A multiple-gaussian fit (red line) gives step sizes of 13.7° ($\sigma = 5.16°$) and −10.9° ($\sigma = 3.9°$) for forward and backward steps, respectively. **b**, The sum of histogram power spectra (see Fig. 3b) for the same data set. Inset, summed spectra of histograms of mean levels between found steps. The forward step size is in close agreement with the peak in the summed spectra, confirming that there are 26 steps per revolution.

METHODS

***E. coli* chimaera.** *E. coli* strain YS34 (Δ*cheY*, *fliC*::Tn*10*, Δ*pilA*, Δ*motAmotB*) was derived from strain RP4979 (ref. 27) (Δ*cheY*) and transformed with plasmids pYS11 (*fliC* sticky filaments[28], ampicillin resistance, pBR322 derivative) and pYS13 (*pomApotB* (ref. 6), isopropyl βD-thiogalactoside inducible, chloramphenicol resistance, pMMB206 derivative). Deletions of *pilA* and *motAB* were made as described in ref. 29; *fliC*::Tn*10* was transduced from HCB1271 (ref. 16). Cells were grown for 5 h at 30 °C from frozen stocks, with shaking, in tryptone broth (TB) containing antibiotics to preserve plasmids. Isopropyl βD-thiogalactoside (1–10 μM) was added for low-level expression of stator proteins.

Rotation measurement. All experiments were performed at 23 °C. Speeds were obtained from power spectra of combined (x,y) data[16], using data windows of length 1 or 4 s beginning at intervals of 0.1 s. Motor angles were obtained by fitting an ellipse to bead trajectories under the assumption that trajectories represent the projection of a circular orbit onto the focal plane of the microscope[18].

For BFP experiments, polystyrene beads (diameter 535 nm; Polysciences) were attached to truncated flagella of immobilized cells, and bead position (x,y) was measured by BFP laser interferometry (sample rate 4 kHz) as described[16]. NaCl (or LiCl) was added to the Na^+-free motility medium in various concentrations; the total concentration of added salt was adjusted to 85 mM with KCl. Custom-made flow chambers allowed a complete exchange of medium in about 5 s.

For fluorescence experiments, fluorescent polystyrene beads (diameter 227 nm, 'yellow/green'; Molecular Probes) were attached as above. A mercury-arc lamp provided epifluorescence excitation (475-nm bandpass) at an intensity of about 1 W cm^{-2}. Images (16 × 16 pixels, each 80 nm square in the sample plane; 505 nm long-pass) were sampled at a frame rate of 2.4 kHz with a cooled, back-thinned, electron-multiplying charge-coupled device camera (iXon DV860-BI, Andor Technology). Bead position was determined with a precision of about 5 nm by a two-dimensional gaussian fit to the bead image.

Step resolution. The relaxation time of a 500-nm bead attached to an elastic hook rotating about an axis 150 nm from its diameter is about 1.1 ms (ref. 30). For a 200-nm bead the time is about 0.15 ms. These times are lower limits assuming no contribution from the flagellar stub[16], and they set upper limits of about 900 and 6,500 to the number of steps that can be detected per second in BFP and fluorescence experiments respectively. Our actual limits were lower, namely about 200 s^{-1} and about 1,000 s^{-1}, respectively. The latter limit was attained by analysis of dwell-time histograms.

Step analysis. A computer algorithm divided angle versus time records into straight-line portions corresponding to episodes of constant average speed. A second algorithm based on the method of J. W. Kerssemakers (personal communication) detected steps as follows. First, an entire episode was divided into two intervals at the point giving the best least-squares fit to a single-step function. Second, an excess of steps (N_{max} per revolution on average) was assigned by repeatedly dividing, as in the first step, the interval containing the largest range of angles in the previous iteration. Third, a 'quality factor' Q was defined for each assigned step as $Q^2 = (x_1 - x_2)^2/[(\mathrm{var.}_1/n_1) + (\mathrm{var.}_2/n_2)]$, where x_i, $\mathrm{var.}_i$ and n_i are the mean angle, the variance and the number of points in an interval, respectively, and $i = 1$ and $i = 2$ indicate intervals immediately before and after a step. The lowest-quality step was removed and adjacent intervals were concatenated, but only if the quality was below a threshold Q_{min}. Last, the previous step was repeated until no steps remained with $Q < Q_{min}$. The accuracy and sensitivity of the algorithm were tested and a suitable value of Q_{min} for each episode was chosen by applying the algorithm to simulated data with $N_o = 10$, 20, 30, 40 and 80 Poisson-distributed steps per revolution and brownian noise and average speed similar to real data.

Received 1 April; accepted 11 July 2005.

1. Berry, R. M. & Armitage, J. P. The bacterial flagella motor. *Adv. Microb. Physiol.* **41,** 291–337 (1999).
2. Berg, H. C. The rotary motor of bacterial flagella. *Annu. Rev. Biochem.* **72,** 19–54 (2003).
3. Thomas, D. R., Morgan, D. G. & DeRosier, D. J. Rotational symmetry of the C ring and a mechanism for the flagellar rotary motor. *Proc. Natl Acad. Sci. USA* **96,** 10134–10139 (1999).
4. Blair, D. F. & Berg, H. C. Restoration of torque in defective flagellar motors. *Science* **242,** 1678–1681 (1988).
5. Berry, R. M., Turner, L. & Berg, H. C. Mechanical limits of bacterial flagellar motors probed by electrorotation. *Biophys. J.* **69,** 280–286 (1995).
6. Asai, Y., Yakushi, T., Kawagishi, I. & Homma, M. Ion-coupling determinants of Na^+-driven and H^+-driven flagellar motors. *J. Mol. Biol.* **327,** 453–463 (2003).
7. Suzuki, H., Yonekura, K. & Namba, K. Structure of the rotor of the bacterial flagellar motor revealed by electron cryomicroscopy and single-particle image analysis. *J. Mol. Biol.* **337,** 105–113 (2004).
8. Lloyd, S. A. & Blair, D. F. Charged residues of the rotor protein FliG essential for torque generation in the flagellar motor of *Escherichia coli*. *J. Mol. Biol.* **266,** 733–744 (1997).
9. Mehta, A. D. *et al.* Myosin-V is a processive actin-based motor. *Nature* **400,** 590–593 (1999).
10. Schnitzer, M. J. & Block, S. M. Kinesin hydrolyses one ATP per 8-nm step. *Nature* **388,** 386–390 (1997).
11. Yasuda, R., Noji, H., Kinosita, K. Jr & Yoshida, M. F_1-ATPase is a highly efficient molecular motor that rotates with discrete 120 degree steps. *Cell* **93,** 1117–1124 (1998).
12. Diez, M. *et al.* Proton-powered subunit rotation in single membrane-bound F_OF_1-ATP synthase. *Nature Struct. Mol. Biol.* **11,** 135–141 (2004).
13. Berg, H. C. in *Cell Motility* Vol. A (eds Goldman, R., Pollard, T. & Rosenbaum, J.) 47–56 (Cold Spring Harbor Press, New York, 1976).
14. Berg, H. C. & Turner, L. Torque generated by the flagellar motor of *Escherichia coli*. *Biophys. J.* **65,** 2201–2216 (1993).
15. Sowa, Y., Hotta, H., Homma, M. & Ishijima, A. Torque-speed relationship of the Na^+-driven flagellar motor of *Vibrio alginolyticus*. *J. Mol. Biol.* **327,** 1043–1051 (2003).
16. Ryu, W. S., Berry, R. M. & Berg, H. C. Torque-generating units of the flagellar motor of *Escherichia coli* have a high duty ratio. *Nature* **403,** 444–447 (2000).
17. Yorimitsu, T. & Homma, M. Na^+-driven flagellar motor of *Vibrio*. *Biochim. Biophys. Acta* **1505,** 82–93 (2001).
18. Yasuda, R., Noji, H., Yoshida, M., Kinosita, K. Jr & Itoh, H. Resolution of distinct rotational substeps by submillisecond kinetic analysis of F_1-ATPase. *Nature* **410,** 898–904 (2001).
19. Liu, J. Z., Dapice, M. & Khan, S. Ion selectivity of the *Vibrio alginolyticus* flagellar motor. *J. Bacteriol.* **172,** 5236–5244 (1990).
20. Fung, D. C. & Berg, H. C. Powering the flagellar motor of *Escherichia coli* with an external voltage source. *Nature* **375,** 809–812 (1995).
21. Armitage, J. P. & Evans, M. C. Control of the protonmotive force in *Rhodopseudomonas sphaeroides* in the light and dark and its effect on the initiation of flagellar rotation. *Biochim. Biophys. Acta* **806,** 42–55 (1985).
22. Neuman, K. C., Chadd, E. H., Liou, G. F., Bergman, K. & Block, S. M. Characterization of photodamage to *Escherichia coli* in optical traps. *Biophys. J.* **77,** 2856–2863 (1999).
23. Samatey, F. A. *et al.* Structure of the bacterial flagellar hook and implication for the molecular universal joint mechanism. *Nature* **431,** 1062–1068 (2004).
24. Samuel, A. D. & Berg, H. C. Torque-generating units of the bacterial flagellar motor step independently. *Biophys. J.* **71,** 918–923 (1996).
25. Meister, M., Lowe, G. & Berg, H. C. The proton flux through the bacterial flagellar motor. *Cell* **49,** 643–650 (1987).
26. Gabel, C. V. & Berg, H. C. The speed of the flagellar rotary motor of *Escherichia coli* varies linearly with protonmotive force. *Proc. Natl Acad. Sci. USA* **100,** 8748–8751 (2003).
27. Scharf, B. E., Fahrner, K. A., Turner, L. & Berg, H. C. Control of direction of flagellar rotation in bacterial chemotaxis. *Proc. Natl Acad. Sci. USA* **95,** 201–206 (1998).
28. Kuwajima, G. Construction of a minimum-size functional flagellin of *Escherichia coli*. *J. Bacteriol.* **170,** 3305–3309 (1988).
29. Datsenko, K. A. & Wanner, B. L. One-step inactivation of chromosomal genes in *Escherichia coli* K-12 using PCR products. *Proc. Natl Acad. Sci. USA* **97,** 6640–6645 (2000).
30. Block, S. M., Blair, D. F. & Berg, H. C. Compliance of bacterial flagella measured with optical tweezers. *Nature* **338,** 514–518 (1989).

Supplementary Information is linked to the online version of the paper at www.nature.com/nature.

Acknowledgements We thank H. Berg and K. Fahrner for the gift of strain HCB1271. The research of R.B., M.L. and A.R. was supported by combined UK research councils through an Interdisciplinary Research Collaboration in Bionanotechnology, that of A.I., M.H. and T.Y. by Grants-in-Aid from the Ministry of Education, Science, Sports, Culture and Technology of Japan, that of M.H. and T.Y. by Soft Nano-Machine Project of JST, and that of Y.S. by JSPS Research Fellowships for Young Scientists.

Author Contributions BFP experiments were performed by Y.S. and A.R., fluorescence experiments by A.R. and M.L., experimental design was by R.B., A.I., A.R. and Y.S., data analysis by R.B., Y.S. and A.R., and strain construction by Y.S., T.Y. and M.H. Y.S. and A.R. contributed equally to this work.

Author Information Reprints and permissions information is available at npg.nature.com/reprintsandpermissions. The authors declare no competing financial interests. Correspondence and requests for materials should be addressed to R.M.B. (r.berry1@physics.ox.ac.uk).